Extreme Mechanics Letters 34 (2020) 100612

Contents lists available at ScienceDirect

Extreme Mechanics Letters

journal homepage: www.elsevier.com/locate/eml

Static and dynamic properties of pre-twisted leaves and stalks with varying chiral morphologies

Zi-Long Zhao [a], Shiwei Zhou [a], Xi-Qiao Feng [b], Yi Min Xie [a,*]

[a] Centre for Innovative Structures and Materials, School of Engineering, RMIT University, Melbourne 3001, Australia
[b] Institute of Biomechanics and Medical Engineering, Department of Engineering Mechanics, Tsinghua University, Beijing 100084, China

ARTICLE INFO

Article history:
Received 20 September 2019
Received in revised form 8 November 2019
Accepted 16 November 2019
Available online 19 November 2019

Keywords:
Twisting chirality
Morphological gradient
Leaves
Stalks
Pre-twisted beams

ABSTRACT

The mechanical properties and biological functions of tissues and organs in plants are closely related to their structural forms. In this study, we have performed systematic measurements and found that the leaves and stalks of several species of emergent plants exhibit morphologies of twisting and gradient chirality. Inspired by the experimental findings, we investigate, both theoretically and numerically, the static bending and vibrational properties of these plant organs. By modeling the leaves and stalks as pre-twisted cantilever beams, the effects of the cross-sectional geometry, loading condition, handedness perversion, twisting configuration, and morphological gradient, on their mechanical behavior are evaluated. Our analysis reveals that both static and dynamic responses of the beams can be easily tuned by changing their structural parameters. For any part of the beams, its chiral morphology has more significant influences on the overall structural performance (e.g., bending stiffness and natural frequencies) if it is closer to the clamped end. This work not only deepens our understanding of the structure–property–function interrelations of chiral plants, but also holds potential applications in the bio-inspired design of innovative devices and structures.

1. Introduction

Through a long history of natural selection, many biological tissues and organs have evolved into elegant architecture with superior mechanical properties [1,2]. Natural materials take a wide diversity of morphologies, such as hierarchies, arrays, spirals, and fractals, which have attracted much attention from the viewpoint of mechanics and materials science [3,4]. Among others, twisting chirality exists in the slender organs of various plants, for examples, the leaves of *Typha orientalis* (Fig. 1A), *Sparganium stoloniferum*, *Acorus calamus*, *Pancratium maritimum*, and *Narcissus poeticus*, the stalks of *Scirpus rosthorni* and *Sagittaria trifolia*, the petals of *Paphiopedilum dianthum*, and the roots of *Arabidopsis* [5–10]. Recently, increasing effort has been directed towards understanding the unusual properties and functions of chiral materials [11–15]. Exploring their unique mechanical behavior can not only deepen our understanding of the structure–property–function interrelations of living systems, but also hold great promise in the bio-inspired design of metamaterials [16–21] and engineering structures such as turbine blades and end-milling cutters [22–24]. It is also noted that many landmark buildings have been constructed into twisting configurations in the past decades, e.g., Shanghai Tower and Cayan Tower [25,26].

In this work, we find that the slender leaves and stalks of some representative emergent plants exhibit different morphologies of twisting and gradient chirality. Although the chirality-dependent properties and functions of living systems have been studied extensively [27], the synergetic effects of twisting chirality and morphological gradient remain elusive. Here we combine experimental, theoretical, and numerical efforts to investigate the static and dynamic properties of the emergent leaves and stalks. First, their chiral morphologies were measured. By modeling the plant organs as multi-piece pre-twisted cantilever beams, a mechanical model is established to derive the analytical solution of their force–deflection relation. Furthermore, the vibration properties of the beams are studied via numerical simulations.

2. Materials and methods

2.1. Morphological measurements

The chiral morphologies of four kinds of representative emergent plants were measured, including the leaves of *Typha orientalis*, *Sparganium stoloniferum*, and *Acorus calamus*, and the stalks of *Sagittaria trifolia*. Fresh mature helophytes were collected in Beijing, China. For each kind of plants, three samples of emergent leaves or stalks were selected for the measurements of chiral configurations. From the base to apex, each sample was cut by a sharp blade into a few pieces with a length of about 0.2 m. For

* Corresponding author.
E-mail address: mike.xie@rmit.edu.au (Y.M. Xie).

https://doi.org/10.1016/j.eml.2019.100612
2352-4316/

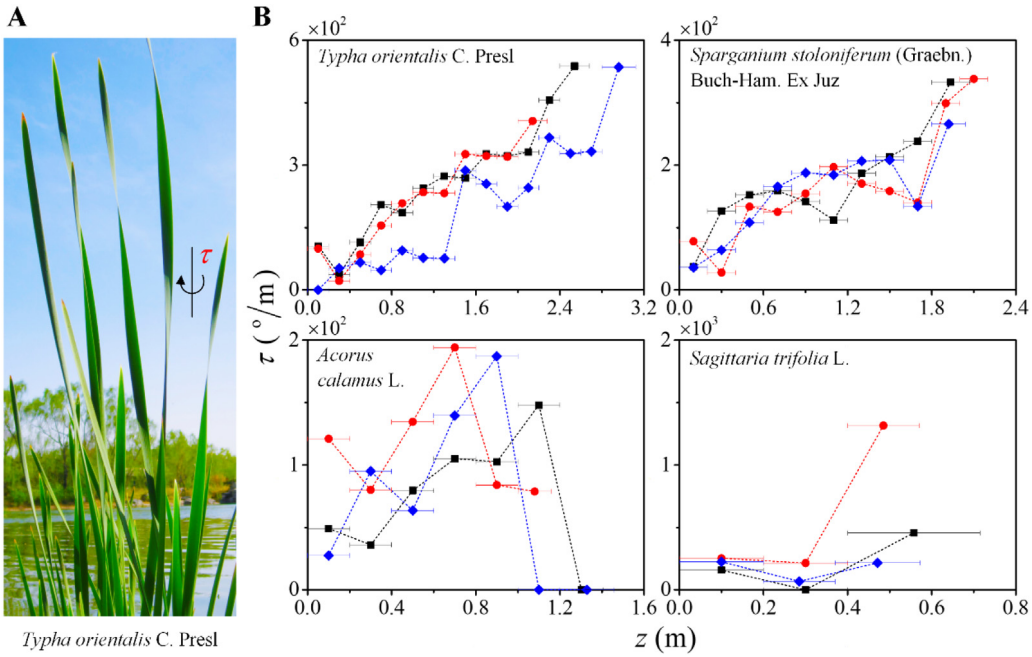

Fig. 1. (A) Leaves of *Typha orientalis*. (B) Variations of the twist τ of four kinds of emergent plants along their length directions.

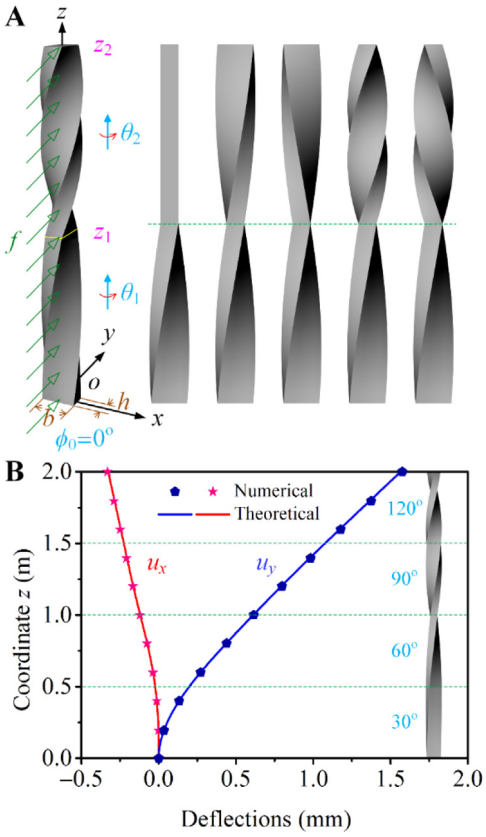

Fig. 2. (A) Illustration of a pre-twisted beam with morphological gradient and two-piece pre-twisted beams with different combinations of twist angles. (B) Variations of the deflections u_x and u_y of a four-piece pre-twisted beam {30°, 60°, 90°, 120°} along the z axis.

each piece, the bottom and top cross-sections and their relative axial rotation were recorded by digital camera. As shown in Fig. 1A, the twist τ of a piece was determined from the magnitude of rotating angle divided by its length. Let z denote the distance between a cross-section and the base of a leaf/stalk. The $\tau - z$ relations of the plants were measured, as shown in Fig. 1B.

2.2. Mechanical model

In the mechanical model, the leaves and stalks are considered as a rectangular cantilever beam consisting of n pieces, where each piece is twisted uniformly along the longitudinal direction. Let b, h, A, and l represent the width, thickness, cross-sectional area, and length of each piece, respectively. The total length of the beam is $L = nl$. Both leaves and stalks are featured by a large slenderness ratio. Along the length direction, the cross-sectional area of the leaves decreases gradually, while that of the stalks is almost a constant. For simplification, we assume that the cross-sectional dimensions b and h of the beams are constant. The rotating angles of the bottom and top cross-section of the ith ($i = 1, 2, \ldots, n$) piece are denoted as ϕ_{i-1} and ϕ_i, respectively. Fig. 2A illustrates the structural parameters of a two-piece pre-twisted beam (for illustration purpose only). Refer to a Cartesian coordinate system (x, y, z), where the origin o is located at the cross-sectional centroid at the clamped end of the beam. When the beam is untwisted and the rotating angle of its bottom surface is $\phi_0 = 0°$, x, y, and z axes are parallel to its width, thickness, and length directions, respectively (Fig. 2A). Assume that the pre-twisted cantilever beam is subjected to a uniformly distributed transverse force f in the y direction, which passes through the neutral axis of the beam, i.e., the z axis.

Fig. 2A also shows several beams with typical combinations of twist angles, where their first pieces have the same twist angle $\theta_1 = 90°$. The twist angles of their second pieces are $\theta_2 = 0°$, $90°$, $-90°$, $180°$, and $-180°$ (from left to right). When $\theta_2 = \theta_1 = 90°$, the two-piece beam is uniformly twisted. The handedness of each piece is described by the sign of its twist angle. For example, $\theta_2 > 0°$ (or $\theta_2 < 0°$) indicates that the second piece is right-handed (or left-handed). The notation $\{\theta_1, \theta_2, \ldots, \theta_n\}$ is introduced to describe the twist angles of a n-piece pre-twisted beam. The deflections of such a beam are analytically solved by our theoretical model. The detailed derivation is given in *Supplementary Material*.

3. Results and discussion

3.1. Varying chiral morphologies

Variations of the twist τ of the four plants along the z direction are plotted in Fig. 1B, where the left and right ends of an error bar indicate the positions of the bottom and top cross-sections of a piece, respectively. The symbols connected by a dash line were measured from an intact leaf or stalk. Fig. 1B shows that the chiral morphologies of all plant organs exhibit a notable gradient along their length directions. The twist τ of *Typha orientalis* and *Sparganium stoloniferum* increases with z in an oscillating manner. Their twisting configurations turn to be very prominent near the apexes (approximately from 500°/m to 600°/m). The twist τ of *Acorus calamus* increases at first and then decreases along the length direction. Their chiral configurations are more prominent in the middle part than in the other parts. By contrast, the $\tau - z$ curves of *Sagittaria trifolia* decrease at first and then increase. Although the short stalks are only about 0.6 m in length, their twist τ can exceed 1300°/m. The four species of helophytes possess distinctly different morphological gradients, which may be related to the loading conditions and their cross-sectional geometries and interior microstructures. Inspired by the above experimental findings, we investigate, both theoretically and numerically, how the twisting and gradient chirality of these plant organs contribute to their structural performance.

3.2. Bending

The bending behavior of pre-twisted cantilever beams is here studied. Unless otherwise specified, we take the following parameters in the examples: length $l = 0.5$ m, width $b = 0.1$ m, thickness $h = 0.05$ m, Young's modulus $E = 1$ GPa, Poisson's ratio $\nu = 0.3$, and force $f = 1$ N/m. The theoretical predictions are first compared with numerical results. In Fig. 2B, the deflections u_x and u_y of a four-piece pre-twisted beam {30°, 60°, 90°, 120°} are plotted as functions of the coordinate z, where the symbols are obtained from finite element analysis (FEA) and the lines are calculated from our mechanical model. The FEA is performed by using Abaqus 6.14. In the numerical simulations, the beam model is discretized by more than 80,000 eight-node hexahedral elements. The beam is clamped at the bottom and free at the top. A body force q is applied on the beam in the y direction, where $q = f/A = 200$ N/m^3. Fig. 2B shows that the theoretical results are in good agreement with the numerical ones.

The influence of the load direction on the structural deformation of uniformly twisted beams is examined. For different twist angles $\theta_1 = 0°$, 90°, 180°, and 360°, the free-end deflections U of the beams are plotted in Fig. 3A and B as a function of the rotating angle ϕ_0 of their bottom surface. We set $b = 2h = 1/10$ m in Fig. 3A and $b = 10h = \sqrt{5}/10$ m in Fig. 3B. Therefore, the beams have the same volume bhL but different cross-sectional aspect ratios b/h. The transverse force f is always in the y direction, and the rotating angle ϕ_0 varies from 0° to 360°. The period of the $U - \phi_0$ curves is 180°, and their phase angle varies with the twist angle θ_1 of the beams. For a straight beam ($\theta_1 = 0°$) with a narrow cross-section (i.e., a large cross-sectional aspect ratio b/h), the deflection is anisotropic and depends strongly on the load direction ϕ_0. The beam will have a much larger deformation when the force f is perpendicular to its wide face (e.g., $\theta_1 = \phi_0 = 0°$) than that in the case when f is perpendicular to the thickness face (e.g., $\theta_1 = 0°$ and $\phi_0 = 90°$). A straight beam would be susceptible to breaking in the flexible direction. The anisotropy of transverse bending of the beams is characterized by the amplitude of the $U - \phi_0$ curves, which decreases substantially with increasing the twist angle θ_1. It can be found that the maximum deflections of the beams increase significantly as b/h increases from 2 to 10. The larger the cross-sectional aspect ratio of the beam, the more significant the effect of twisting chirality on its anisotropy of transverse bending. It is worth mentioning that the static bending responses of a beam are independent of the twisting configuration if it has a square cross-section ($b/h = 1$).

The effect of the structural handedness on the bending response of a pre-twisted beam is also investigated. Consider a uniformly twisted beam as an example. Fig. 3C and 3D show the variations in U_x and U_y with respect to the twist angle θ_1, where U_x and U_y are the free-end deflections of the beam along the x and y directions, respectively. We set $b = 2h = 1/10$ m in Fig. 3C and $b = 10h = \sqrt{5}/10$ m in Fig. 3D. The deflection U_y, independent of the sign of θ_1 (i.e., the handedness of the beam), decreases monotonously with the increase in $|\theta_1|$. As the twist angle $|\theta_1|$ increases, the magnitude of the deflection U_x increases at first and then decreases. In contrast to the $U_y - \theta_1$ relation, changes in the sign of the twist angle θ_1 lead to a different deflection U_x. Therefore, the $U_x - U_y$ relations of pre-twisted beams can be tuned by changing their structural handedness.

Variation of the free-end deflection U of the two-piece beam with respect to θ_1 is further plotted in Fig. 3E, where we take several representative values of θ_2. As $|\theta_1|$ increases, the $U - \theta_1$ curve decreases rapidly at first (especially for $|\theta_1| < 180°$) and then approaches gradually to a constant. The reduction of the deflection U reaches approximately 1/3 (from 0.12 mm to 0.08 mm) as $|\theta_1|$ increases from 0° to 180°. Fig. 3F shows the bending stiffness S of the two-piece pre-twisted beam. It can be seen that twisting a beam into a chiral configuration can improve its bending stiffness substantially. In comparison to the twist angle θ_2, the influence of θ_1 on the bending stiffness S is much more significant.

3.3. Vibration

The vibration properties of pre-twisted cantilever beams are investigated via FEA. Consider two types of beams, which have a square ($b = h = \sqrt{2}/20$ m) and a rectangular cross-section ($b = 10h = \sqrt{5}/10$ m), respectively. The length and mass density of both beams are set as $L = 2$ m and $\rho = 1000$ kg/m^3, respectively. The beams have the same volume and mass. The first five mode shapes of the two beams are shown in Fig. 4, where the transparent meshes and solid structures represent the undeformed and deformed configurations, respectively. In each plot, the color varies from blue to red as the magnitude of flexural displacement increases. The beams are placed in the horizontal direction in Fig. 4, which is for illustration purpose only. The slender beam with a square cross-section has only bending deformation in the first five mode shapes (Fig. 4A and B). Twisting the square beam into a chiral configuration does not change its mode shapes. The straight beam with a narrow cross-section ($b/h = 10$) undergoes axial torsion in the 4 th mode (Fig. 4C). It is much easier to bend the beam in its thickness direction than in its width direction. Therefore, the beam is bent along its flexible direction in the first two modes. It is noted that the mode shapes of the narrow beam depends strongly on its twisting configuration. The mode shapes of the pre-twisted beam in Fig. 4D are distinctly different from those in Fig. 4C, but similar to the shapes in Fig. 4A and B.

Further, the first five natural frequencies ω_i ($i = 1, 2, \ldots, 5$) of the two beams are calculated and compared by using FEA (Fig. 5A). For the square beam, $\omega_1 = \omega_2$ and $\omega_3 = \omega_4$. The natural frequencies of the beam are independent of the twisting configuration (i.e., $\mathrm{d}\omega_i/\mathrm{d}\theta_1 = 0$, $i = 1, 2, \ldots, 5$). For the beam with a narrow cross-section, its natural frequencies vary significantly with the twist angle θ_1. When θ_1 increases to a large

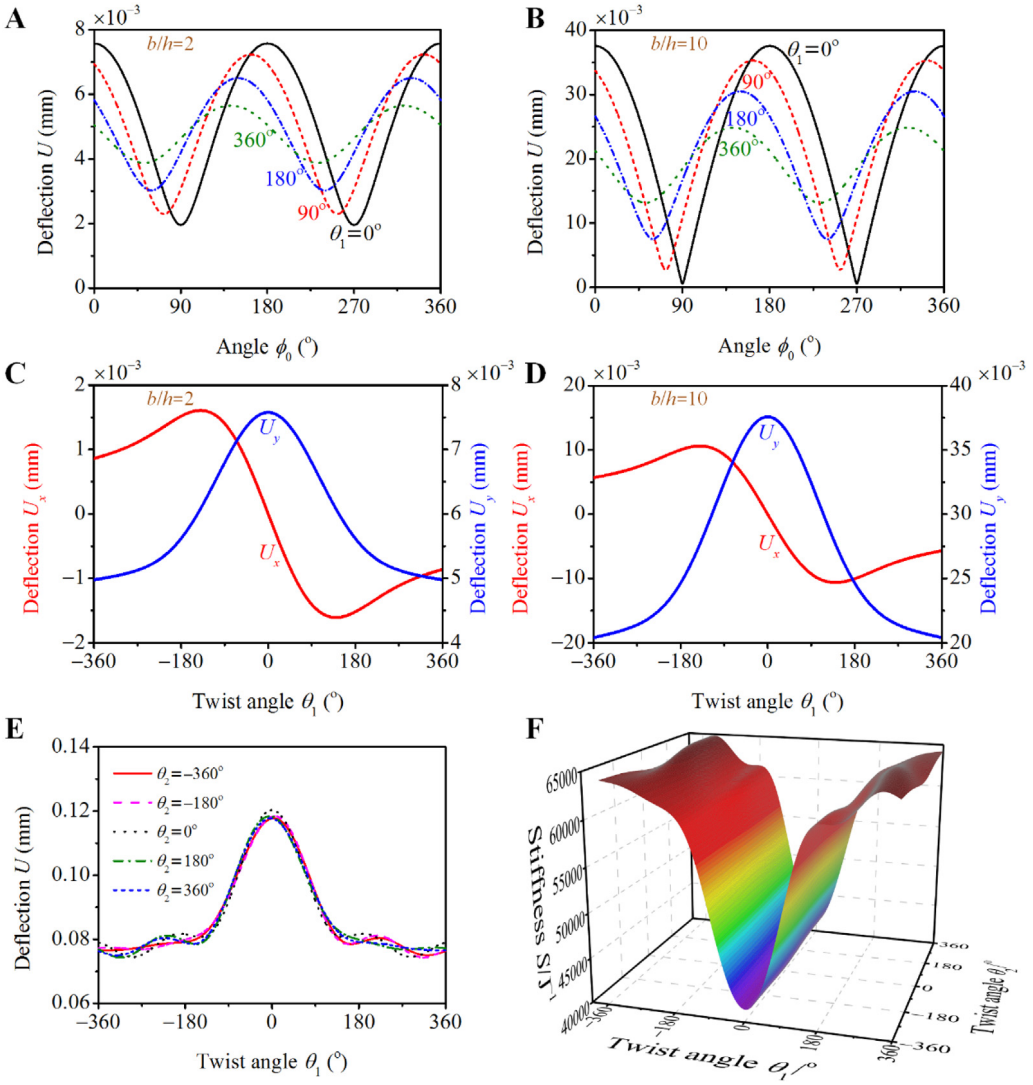

Fig. 3. Variations of the free-end deflection U of uniformly pre-twisted beams with respect to the load direction ϕ_0, where b/h is set as 2 in (A) and 10 in (B). Free-end deflections U_x and U_y of uniformly pre-twisted beams as a function of the twist angle θ_1, where b/h is set as 2 in (C) and 10 in (D). (E) $U-\theta_1$ relations of a two-piece pre-twisted beam. (F) Structural stiffness S of the beam as a function of the twist angles θ_1 and θ_2.

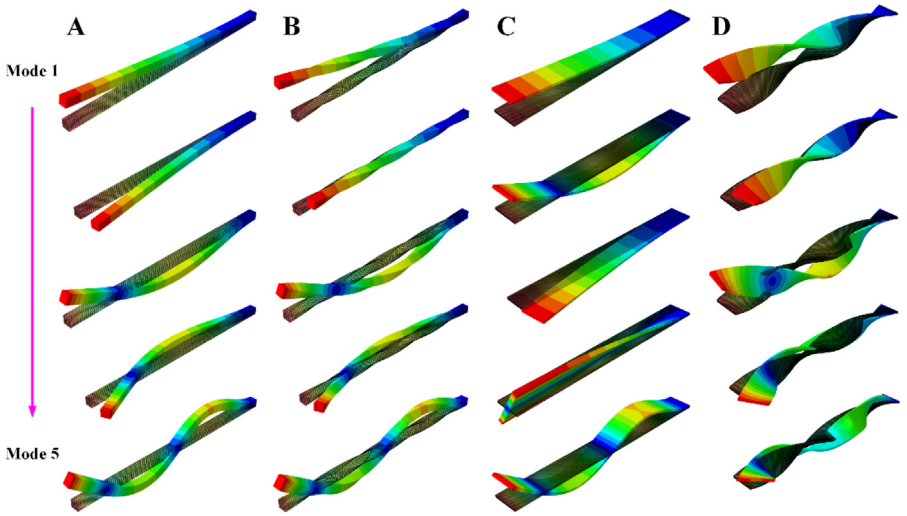

Fig. 4. First five mode shapes of two kinds of beams, where b/h is 1 in (A) and (B), and 10 in (C) and (D). The beam in (A) and (C) is straight, while the beam in (B) and (D) twists 360° uniformly along its length direction.

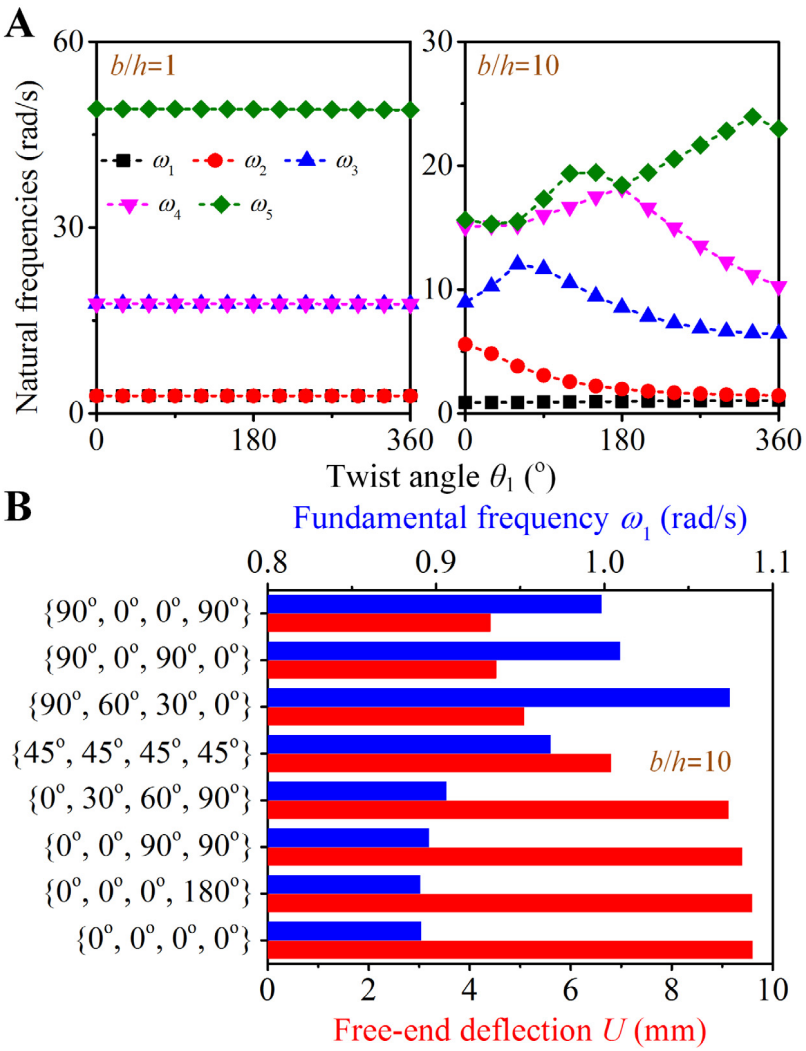

Fig. 5. (A) Variations of natural frequencies of uniformly twisted beams with respect to their twist angle θ_1. (B) Free-end deflections U and fundamental frequencies ω_1 of four-piece pre-twisted beams with different combinations of twist angles.

value (e.g., 360°), the transverse bending anisotropy of the pre-twisted beam turns to be very small, and ω_2 approaches to the fundamental frequency ω_1. When θ_1 increases from 0° to 360°, ω_1 is increased by as large as 18% (from 0.89 rad/s to 1.05 rad/s).

The effects of the morphological gradient of the multi-piece beams on their free-end deflection U and fundamental frequency ω_1 are investigated (Fig. 5B). The pre-twisted beams have four pieces and twist 180° in total along the z direction, where we take different combinations of twist angles. It is found that although the total twist angle remains unchanged, adjusting the combinations of $\{\theta_1, \theta_2, \theta_3, \theta_4\}$ can result in distinctly different mechanical responses of the beam. For example, the deflection of the beam {90°, 0°, 0°, 90°} is less than half of that of the straight beam {0°, 0°, 0°, 0°}. Compared with the straight beam {0°, 0°, 0°, 0°}, the frequency ω_1 of the beam {90°, 60°, 30°, 0°} is increased by 20% (from 0.89 rad/s to 1.07 rad/s). However, the pre-twisted beam {0°, 0°, 0°, 180°} and the straight beam {0°, 0°, 0°, 0°} have almost the same deflection and fundamental frequency, although the former has a prominent chiral morphology.

3.4. Discussion

According to our observations, the leaves of emergent plants have very narrow cross-sections (e.g., Fig. 1A). Emergent leaves with limited materials generally seek to maximize their slenderness ratio L/A and surface-area-to-volume ratio $\lambda = 2(b+h)/A$, where the cross-sectional area A is assumed to be a constant for a specific leaf. The upright-standing, slender configurations enable the leaves to adapt to water-level fluctuations. Note that $d\lambda/d\mu = \left(1 - A/b^2\right)/b \geq 0$, where $\mu = b/h$ is the cross-sectional aspect ratio. Leaves with a narrower cross-section will have a larger surface-area-to-volume ratio, which is important for them to gain sufficient sunlight for photosynthesis. However, the large slenderness ratio and cross-sectional ratio will lead to notable drag force when the leaves are exposed to wind in the flexible direction. By contrast, the stalks of emergent plants have a relative thick cross-section ($1 \leq \mu \leq 2$) such that they can support head organs. Fig. 3A and B show that the twisting configurations can help these plant organs to accommodate wind forces coming from different directions, and thus help them realize important biological functions.

Further, our results reveal that the morphological gradient of the plant organs also plays an important role in determining their mechanical properties. First, both static and dynamic responses, e.g., deflections and mode shapes, of the beams can be easily adjusted by controlling their structural parameters such as cross-sectional geometries and twisting configurations. Secondly, a gradient design could have much better structural performance than the uniformly twisted design (Fig. 5B). Thirdly, the handedness

perversion could greatly influence the coupled $U_x - U_y$ relation of the pre-twisted beams. Fourthly, for any part of the beams, its chiral morphology would have more significant influences on the overall structural performance (e.g., bending stiffness and natural frequencies) if it is closer to the clamped end (e.g., Figs. 3E and 5B). It is worth mentioning that perversion is widely observed in chiral biological materials such as plant tendrils, which can be divided into two pieces of opposite handednesses [28–30]. This geometric phenomenon is not observed in the leaves and stalks of the four helophytes. Nevertheless, the handedness perversion has here been proved to be an effective approach for adjusting the coupled $U_x - U_y$ relation of pre-twisted beams (Fig. 3C and D), which holds potential applications in the optimal design of chiral structures.

4. Conclusions

In summary, we have performed systematic measurements and found that the leaves and stalks of emergent plants exhibit different morphologies of gradient twisting chirality. Both static and dynamic properties of these slender organs have been investigated through a combination of theoretical and numerical analyses. The results reveal the structure–property–function interrelations of the plant organs, as well as the synergistic effects of their twisting chirality and morphological gradient. It is found that the mechanical responses of the leaves and stalks are closely related to the loading conditions and their structural parameters such as twist angles and cross-sectional aspect ratios. The presented results are directly applicable to the optimal design of pre-twisted beams. The chirality-dependent and easily tunable elastic properties of this kind of beams are of significant importance for their applications in, for instance, innovative devices and structures, and high-rise buildings subjected to lateral loading including earthquake and wind.

Acknowledgments

Supports from the Australian Research Council (DP160101400) and the National Natural Science Foundation of China (11432008) are acknowledged.

Appendix A. Supplementary data

Supplementary material related to this article can be found online at https://doi.org/10.1016/j.eml.2019.100612.

References

[1] M.A. Meyers, P.Y. Chen, A.Y.M. Lin, Y. Seki, Biological materials: Structure and mechanical properties, Prog. Mater. Sci. 53 (2008) 1–206.
[2] P.Y. Chen, J. McKittrick, M.A. Meyers, Biological materials: Functional adaptations and bioinspired designs, Prog. Mater. Sci. 57 (2012) 1492–1704.
[3] D.W. Thompson, On Growth and Form, Cambridge University Press, 1942.
[4] Z.L. Zhao, S. Zhou, X.Q. Feng, Y.M. Xie, On the internal architecture of emergent plants, J. Mech. Phys. Solids 119 (2018) 224–239.
[5] Z.L. Zhao, et al., Biomechanical tactics of chiral growth in emergent aquatic macrophytes, Sci. Rep. 5 (2015) 12610.
[6] Z.L. Zhao, Z.Y. Liu, X.Q. Feng, Chirality-dependent flutter of *Typha* blades in wind, Sci. Rep. 6 (2016) 28907.
[7] K. Schulgasser, A. Witztum, Spiralling upward, J. Theoret. Biol. 230 (2004) 275–280.
[8] J. Liu, et al., The structure and flexural properties of *Typha* leaves, Appl. Bionics Biomech. 2017 (2017) 1249870.
[9] J. Liu, et al., Experimental study and numerical simulation on the structural and mechanical properties of *Typha* leaves through multimodal microscopy approaches, Micron 104 (2018) 37–44.
[10] H. Wada, D. Matsumoto, Twisting growth in plant roots, in: Plant Biomechanics, Springer, 2018, pp. 127–140.
[11] R. Oda, I. Huc, M. Schmutz, S. Candau, F. MacKintosh, Tuning bilayer twist using chiral counterions, Nature 399 (1999) 566–569.
[12] J. Foroughi, et al., Torsional carbon nanotube artificial muscles, Science 334 (2011) 494–497.
[13] S.J. Gerbode, J.R. Puzey, A.G. McCormick, L. Mahadevan, How the cucumber tendril coils and overwinds, Science 337 (2012) 1087–1091.
[14] J. Yuan, P. Poulin, Fibers do the twist, Science 343 (2014) 845–846.
[15] C.S. Haines, et al., New twist on artificial muscles, Proc. Natl. Acad. Sci. USA 113 (2016) 11709–11716.
[16] T. Frenzel, M. Kadic, M. Wegener, Three-dimensional mechanical metamaterials with a twist, Science 358 (2017) 1072–1074.
[17] W. Chen, D. Ruan, X. Huang, Optimization for twist chirality of structural materials induced by axial strain, Mater. Today Commun. 15 (2018) 175–184.
[18] W. Wu, et al., Compression twist deformation of novel tetrachiral architected cylindrical tube inspired by towel gourd tendrils, Extreme Mech. Lett. 20 (2018) 104–111.
[19] W. Chen, X. Huang, Topological design of 3D chiral metamaterials based on couple-stress homogenization, J. Mech. Phys. Solids 131 (2019) 372–386.
[20] C. Ma, et al., Experimental and simulation investigation of the reversible bi-directional twisting response of tetra-chiral cylindrical shells, Compos. Struct. 203 (2018) 142–152.
[21] L.Y. Zhang, Z.L. Zhao, Q.D. Zhang, X.Q. Feng, Chirality induced by structural transformation in a tensegrity: Theory and experiment, J. Appl. Mech. 83 (2016) 041003.
[22] W.R. Chen, Parametric studies on bending vibration of axially-loaded twisted Timoshenko beams with locally distributed Kelvin–Voigt damping, Int. J. Mech. Sci. 88 (2014) 61–70.
[23] W.R. Chen, C.S. Chen, Parametric instability of twisted Timoshenko beams with localized damage, Int. J. Mech. Sci. 100 (2015) 298–311.
[24] D. Adair, M. Jaeger, Vibration analysis of a uniform pre-twisted rotating Euler–Bernoulli beam using the modified Adomian decomposition method, Math. Mech. Solids 23 (2018) 1345–1363.
[25] J.W. Tang, Y.M. Xie, P. Felicetti, J.Y. Tu, J.D. Li, Numerical simulations of wind drags on straight and twisted polygonal buildings, Struct. Design Tall Spec. Build. 22 (2013) 62–73.
[26] P. Nikandrov, Evolution tower, Moscow: Upward spiral: The story of the evolution tower, CTBUH J. (2016) 12–19.
[27] Z.L. Zhao, et al., Synergistic effects of chiral morphology and reconfiguration in cattail leaves, J. Bionic Eng. 12 (2015) 634–642.
[28] A. Goriely, M. Tabor, Spontaneous helix hand reversal and tendril perversion in climbing plants, Phys. Rev. Lett. 80 (1998) 1564.
[29] T. McMillen, A. Goriely, Tendril perversion in intrinsically curved rods, J. Nonlinear Sci. 12 (2002) 241–281.
[30] J.S. Wang, et al., Hierarchical chirality transfer in the growth of towel gourd tendrils, Sci. Rep. 3 (2013) 3102.